

Transport properties of the transverse charge-density-wave system $\text{Fe}_3\text{O}_2\text{BO}_3$

J. C. Fernandes, R. B. Guimarães, and M. A. Continentino*
Instituto de Física, Universidade Federal Fluminense, Niterói, RJ, 24.210-340 Brazil

E. C. Ziemath and L. Walmsley
*Departamento de Física—IGCE—Rio Claro, Universidade Estadual Paulista—UNESP, Rua 10, 2527—Bairro Santana—
 CEP 13500-230—Rio, Claro—SP, Brazil*

M. Monteverde
*Consejo Nacional de Investigaciones Científicas y Técnicas Laboratorio de Bajas Temperaturas, Departamento de Física—
 FCEyN—UBA, Ciudad Universitaria, PAB I (C1428EHA) Buenos Aires, Argentina*

M. Núñez-Regueiro
Centre de Recherches sur Les Tres Basses Temperatures, CNRS, BP166, 38042 Grenoble Cedex 9, France

J.-L. Tholence and J. Dumas
Laboratoire d'Etudes des Propriétés Electroniques des Solides, CNRS, BP 166, 38042 Grenoble, Cedex 9, France
 (Received 16 February 2005; published 24 August 2005)

We study the transport properties of the charge-density-wave system $\text{Fe}_3\text{O}_2\text{BO}_3$. ac conductivity measurements for different frequencies are presented for temperatures above and below the structural transition. dc conductivity, as a function of temperature and pressure, yields the variation of the transition temperature with external pressure. Below this transition the conductivity is thermally activated in a wide range of temperature and the gap obtained is strongly pressure dependent. The ac conductivity at sufficiently low temperatures below the transition is ascribed to the excitation of local defects associated with domain walls and which are characteristic of the one-dimensional nature of the $\text{Fe}_3\text{O}_2\text{BO}_3$ system.

DOI: [10.1103/PhysRevB.72.075133](https://doi.org/10.1103/PhysRevB.72.075133)

PACS number(s): 71.45.Lr, 77.22.Gm, 71.35.Lk, 72.60.+g

I. INTRODUCTION

In low-dimensional structures, such as ladders, we may find distortions generating transverse charge-density waves (CDW). This was recently observed¹ in the oxy-borate system $\text{Fe}_3\text{O}_2\text{BO}_3$. This ludwigite has in its structure subunits in the form of three leg ladders (3LL), which become unstable with decreasing temperature. Each rung in the 3LL consists of three Fe^{3+} ions with one extra electron spread along the rung. The instability is such that the rungs dimerize in alternate directions *perpendicular* to the axis of the ladder as shown in Fig. 1. For the dimerized rungs, the electronic charge density is greater between the nearest ions.³ The structural transition at $T_S \approx 283$ K is accompanied by a change in the activation energy of the electrical resistivity.¹ An important distinction between the $\text{Fe}_3\text{O}_2\text{BO}_3$ ludwigite and the common Peierls systems is the existence of local moments belonging to the Fe ions which interact with the CDW; besides, the mechanism responsible for the CDW formation is different from that of the Peierls distortion in one-dimensional metals.² Here we are dealing with an excitonic instability due to the coupling between an empty band and a fully occupied one.³

Previous magnetic studies on $\text{Fe}_3\text{O}_2\text{BO}_3$ shows the onset of magnetic order at $T_{N1} = 112$ K, as seen by Mössbauer spectroscopy,⁴ and a transition to a weak ferromagnetic phase at $T_{N2} = 70$ K associated with a sharp peak in the ac susceptibility.⁵ The maximum of the ac-susceptibility curve, at T_{N2} , has a negligible frequency dependence implying that,

in spite of some competition, this is indeed a magnetic phase transition and not a progressive freezing of the magnetic moments.

The magnetic character of the ions involved in the charge-density wave led Whangbo *et al.*⁶ to suggest a magnetic mechanism as the cause of the structural instability of $\text{Fe}_3\text{O}_2\text{BO}_3$. This material, in fact, presents a behavior similar to both spin-Peierls (SP) and more conventional Peierls systems. The BCS ratio $2\Delta/k_B T_S$ is anomalous³ in common with the latter. In SP systems this is much closer to the mean-field theoretical value of ≈ 3.52 . In this paper, we will focus mostly on the charge aspects of the problem where the itinerant electrons play the main role. We present ac-conductivity measurements in single crystals of $\text{Fe}_3\text{O}_2\text{BO}_3$ at different frequencies and temperatures with the electrical field *perpendicular* to the 3LL direction (*c* axis). We find that below the structural transition temperature T_S the frequency-dependent conductivity may be described by a damped oscillator model whose characteristic frequency ω_0 , however, is too large to be reached in the present experiments.⁷ A model is suggested to explain this behavior. For temperatures much below T_S the real part of the conductivity increases with increasing frequency. Also the imaginary part of the conductivity varies linearly with frequency at the highest frequencies. The ladder structure, the nature of the distorted phase, and the geometry of the ac-experiments suggest that the observed behavior is due to oscillating charges that are associated with domain walls. We also present dc-conductivity measurements on single crystals of the same compound, as a

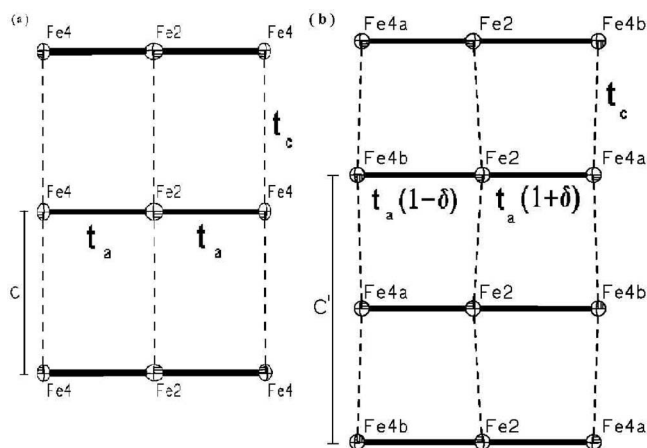


FIG. 1. Schematic structure of the 3LL in $\text{Fe}_3\text{O}_2\text{BO}_3$ ludwigite before and after the dimerization transition (from Ref. 3).

function of hydrostatic pressure, with the current *parallel* to the 3LL direction. Our results show that the structural instability shifts to lower temperatures in the presence of the applied pressure but for high enough pressures it becomes very wide. Below the transition temperature T_S the dc conductivity is thermally activated with a gap that decreases with increasing pressure.

II. EXPERIMENT

A. ac Conductivity

The samples used in this study were prepared as described in Ref. 5. The conductivity versus frequency measurements were performed in the frequency range 100 Hz–1 MHz on a prismatic single crystal of $\text{Fe}_3\text{O}_2\text{BO}_3$ measuring $0.227 \times 0.82 \times 1.8 \text{ mm}^3$. The latter longer length corresponds to the c axis of the material. This crystal was placed inside a parallel-plate circular capacitor with its largest faces in contact with the capacitor plates whose diameter was 4.0 mm, such that, the electric field is perpendicular to the c axis. This partially filled capacitor was inside a cryostat JANIS model CCS-150. The module and argument δ of its total impedance Z was measured as a function of frequency by a SOLARTRON Impedance Analyzer, model 1260. The real and imaginary parts of the sample conductivity, σ_R and σ_I are shown in Fig. 2 and 3. Figure 4 shows some isotherms of $\epsilon(\omega)/\epsilon_0$ as a function of frequency where the dielectric constant $\epsilon(\omega) = (\sigma_I/\omega)$.

B. dc Conductivity

The electrical resistivity measurements were performed in a sintered diamond Bridgman anvil apparatus using a pyrophyllite gasket and two steatite disks as the pressure medium. The Cu-Be device that locked the anvils can be cycled between 4 K and 300 K in a sealed dewar. Pressure was calibrated against the various phase transitions of Bi under pressure at room temperature and by a superconducting Pb manometer at a low temperature. The overall uncertainty in the quasihydrostatic pressure is estimated to be $\pm 15\%$. The

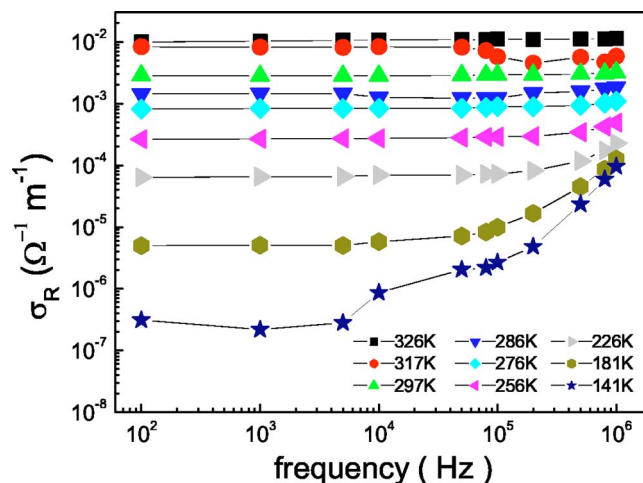


FIG. 2. (Color online) Real part of the conductivity of the $\text{Fe}_3\text{O}_2\text{BO}_3$ ludwigite as a function of frequency for several temperatures.

pressure spread across the sintered diamond anvils was previously determined on Pb manometers to be of about 1.5–2 GPa depending on the applied pressure. The temperature was determined using a calibrated carbon glass thermometer with a maximum uncertainty (due mainly to temperature gradients across the Cu-Be clamp) of 0.5 K. Four probes of electrical resistivity measurements were made by using platinum wires to make contact on the sample and using a Keithley 2182 nanovoltmeter combined with a Keithley 220 current source. Special care was taken to avoid Joule heating of the highly resistive samples. In Fig. 5, we show the logarithm of the resistance as a function of inverse temperature. For different pressures and in a large temperature range, the resistance is thermally activated. We show in the inset the way in which we obtain the transition temperatures (T_S) and the gap Δ . The former are obtained as extrema in the plots of the derivative

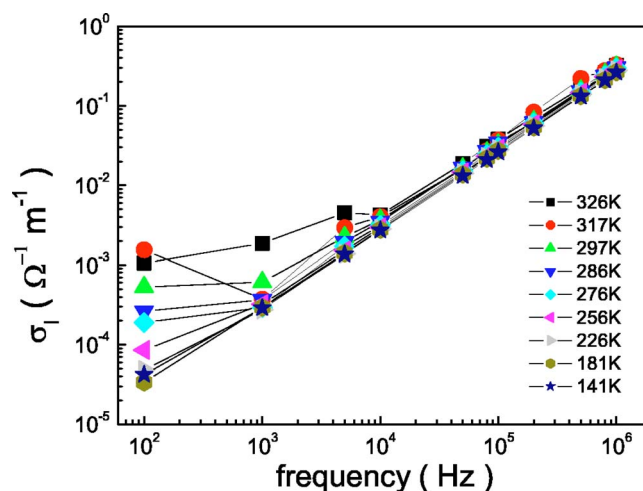


FIG. 3. (Color online) Imaginary part of the conductivity of the $\text{Fe}_3\text{O}_2\text{BO}_3$ ludwigite as a function of frequency for different temperatures. For temperatures below the structural transition temperature T_S and high frequencies σ_I presents a linear frequency dependence, $\sigma_I = 3.27 \times 10^{-4} + 4.22 \times 10^{-8} \omega$.

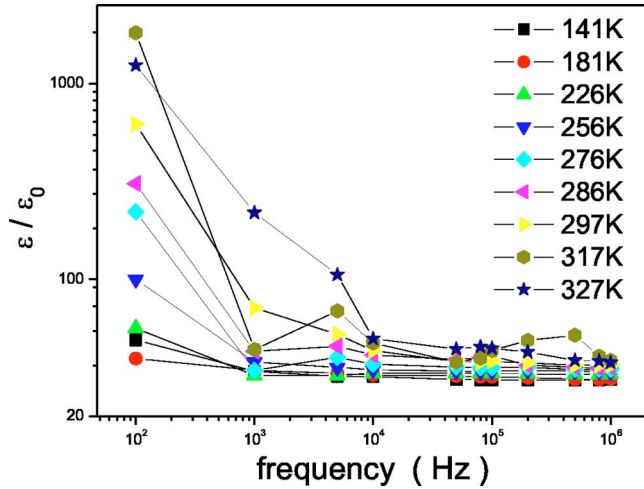


FIG. 4. (Color online) Real part of the dielectric constant of the $\text{Fe}_3\text{O}_2\text{BO}_3$ ludwigite as a function of frequency for different temperatures.

of the logarithm of the resistance with respect to inverse temperature versus inverse temperature, while the pressure-dependent gap corresponds to the plateau in these curves for $T < T_S$. Unfortunately, for the higher pressures the peak defining T_S is washed away as the transition becomes too broad, and we can only determine Δ . In Fig. 6 we show the evolution of these two parameters with pressure. We find that for low applied pressures $dT_S/dP \approx -1$ K/kbar which is not very different from values found in some CDW materials.⁸

III. DISCUSSION

The structural phase transition in $\text{Fe}_3\text{O}_2\text{BO}_3$ clearly appears in the dc-transport measurements as anomalies in the

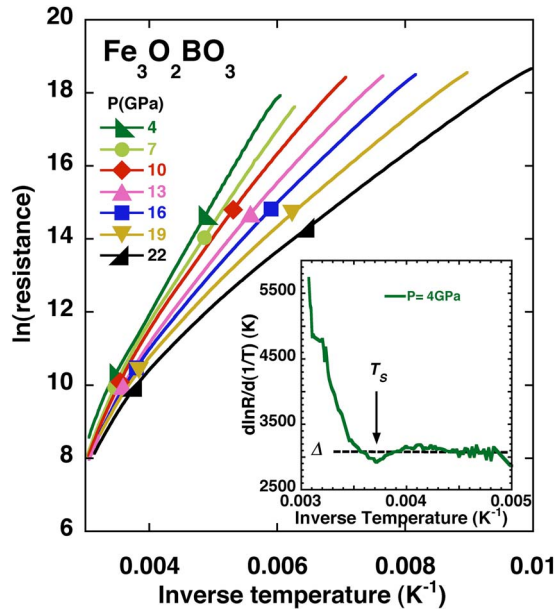


FIG. 5. (Color online) Logarithm of the electrical resistance as a function of inverse temperature for different pressures. Inset: view of the logarithmic derivative with respect to inverse temperature for the first pressure showing the way for obtaining the gap Δ and the transition temperature T_S .

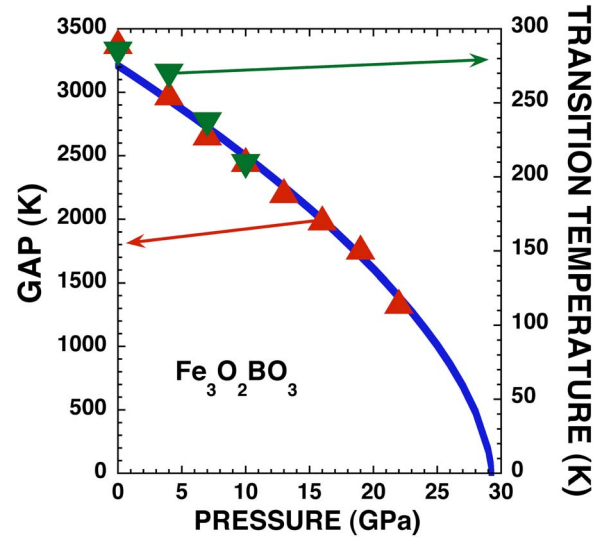


FIG. 6. (Color online) Evolution of the gap Δ (Δ) and the transition temperature T_S (∇) with pressure. The solid line corresponds to a fit to both Δ and T_S using a power law, $T_S \propto \Delta \propto |P_C - P|^{0.6}$.

logarithmic derivative of the conductivity. These anomalies are pressure dependent and allow us to trace the behavior with respect to pressure of the temperature of the structural transition. On the other hand, the ac conductivities present distinct behaviors at different temperatures that we now discuss. In the real part of the conductivity, the most interesting feature besides some low frequency anomalies for T close to T_S is the increase with frequency of $\sigma_R(\omega)$ especially at low temperatures. In the imaginary part of the conductivity, this behavior is accompanied by the appearance of a component proportional to frequency which extends to lower frequencies as T is reduced. In order to interpret these results, it is important to consider the crystal structure of the ludwigites, specifically the three leg ladders. Also we have to consider the geometry of the experiments with the oscillating electric field applied perpendicularly to the ladders.

The rise of $\sigma_R(\omega)$ with frequency at low temperatures is clearly associated with the CDW formation below the structural phase transition. The CDW, shown in Fig. 1, has two possible configurations which can be interchanged by a mirror reflection through a plane perpendicular to the 3LL plane. If the number of rungs is even, both configurations have the same energy under a dc electrical field applied in the plane of the 3LL and perpendicularly to the charge-density-wave direction. However, if this number is odd (see Fig. 7), the energies are different for each configuration. In a real material these two configurations coexist separated by domain walls, and it is much more favorable energetically for the perpendicular electric field to act in these domain walls or defects instead of acting in a whole domain, as shown in Fig. 7.

The σ_R and σ_I versus ω isotherms at low temperatures clearly exhibit anomalies with general features of the complex conductivity of coherent oscillating charges.⁹ Let us estimate the mass and the spring constant for the oscillator generating these anomalies. The real and imaginary parts of the complex conductivity, for charges moving as harmonic oscillators, are

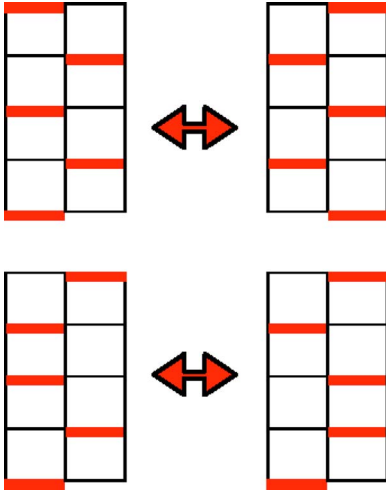


FIG. 7. (Color online) Possible configurations of the dimerized 3 LL. The bold line is the short bond (see Fig. 1). On top we show two configurations which are degenerate in the absence of a perpendicular electric field. On the bottom we show a defect, which is characterized by two adjacent distorted bonds. This is essentially a domain wall between two degenerate configurations. Note that in this case it is sufficient that one bond jumps for the system to move from one configuration to another.

$$\sigma_R = \frac{ne^2\tau}{m} \frac{\omega^2/\tau^2}{(\omega_0^2 - \omega^2)^2 + \omega^2/\tau^2}, \quad (1)$$

and

$$\sigma_I = \frac{ne^2\tau}{m} \frac{(\omega_0^2 - \omega^2)\omega/\tau}{(\omega_0^2 - \omega^2)^2 + \omega^2/\tau^2}. \quad (2)$$

For frequencies and temperatures, such that $\omega/\omega_0 \ll 1$ and $\omega_0\tau_R \leq 1$ [$\tau_R = 1/(\omega_0^2\tau)$], the imaginary part of the conductivity can be written as $\sigma_I(\omega) \approx (ne^2/m\omega_0^2)\omega$. This increases linearly with a frequency with a coefficient that is essentially temperature independent. In Fig. 3 we can observe this behavior, which sets in at lower frequencies as temperature is decreased. The coefficient of the straight line in Fig. 3 yields $(ne^2/m\omega_0^2) = 4.22 \times 10^{-8} \Omega^{-1} \text{m}^{-1} \text{s}$. Notice that in these equations n is the number of oscillators per unit volume and m their mass. The spring constant $K = m\omega_0^2$. Another useful relation valid for $\omega/\omega_0 \ll 1$ that involves σ_R is given by $[\sigma_R(\omega) - \sigma_R(0)]/\sigma_I(\omega) = \omega\tau_R$. Figure 8 shows that indeed at low temperatures and high frequencies $[\sigma_R(\omega) - \sigma_R(0)]/\sigma_I(\omega)$ is linear in frequency and the nearly constant slope yields a temperature-independent relaxation time $\tau_R \sim 10^{-10} \text{ s}$. The ac-conductivity results then imply the existence in $\text{Fe}_3\text{O}_2\text{BO}_3$ of oscillators with a characteristic frequency ω_0 in the range $10^8 - 10^{10} \text{ Hz}$, such that, the conditions $\omega/\omega_0 \ll 1$ and $\omega_0\tau_R \leq 1$ are fulfilled. We associate these oscillators with the defects or domain walls described above and shown in Fig. 7. The numerical results obtained above put some constraints on the mass of these defects. From Fig. 3, $ne^2/m\omega_0^2 = 4.22 \times 10^{-8} \Omega^{-1} \text{m}^{-1} \text{s}$. Since n is a fraction of the total number N of Fe^{3+} or of rungs in the ladders, this can be written as $n = cN$ where c is the concentration of defects.

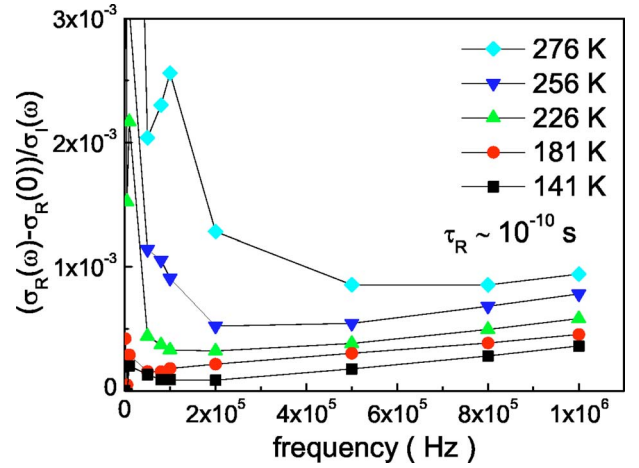


FIG. 8. (Color online) Ratio between real and imaginary parts of conductivity. It can be seen that at high frequencies and low temperatures this quantity increases linearly with frequency with a weakly temperature dependent slope (see text).

Using¹⁰ $N = 1.47 \times 10^{28} \text{ m}^{-3}$, $c = 10^{-3}$ as estimated from electron paramagnetic resonance Fe^{3+} line intensity observed for $120 \text{ K} < T < 200 \text{ K}$ (Ref.11) and taking $\omega_0 \sim 10^{10} \text{ s}^{-1}$, we obtain $m \approx 10^5 \times m_e$ where m_e is the electron mass. On the other hand, with $\omega_0 = 10^8 \text{ s}^{-1}$ we get the unreasonable large value $m \approx 10^9 \times m_e$. Notice also that with the characteristic frequency of order $\omega_0 = 10^{10} \text{ s}^{-1}$ the condition $\omega_0\tau_R \leq 1$ required above is satisfied for τ_R of order 10^{10} s as obtained in Fig. 8. Summing up our ac experiments are consistent with the existence of oscillating charges with a characteristic frequency $\omega_0 \sim 10^{10} \text{ s}^{-1}$ and relaxation times $\tau \sim \tau_R \sim 10^{-10} \text{ s}$, which are nearly temperature independent from T_S down to $\sim 140 \text{ K}$. These oscillators are identified with defects which are domain walls between the two degenerate configurations of the transverse charge-density waves.

The dc measurements show that below the structural transition and down to the lowest temperatures of the measurements ($\sim 140 \text{ K}$), the conductivity is thermally activated. The structural transition, as well as the conductivity gap, decrease with increasing pressure. We observe a pressure-independent relation between the gap and the transition temperature, $2\Delta/k_B T_S = 23$, that is clearly nonmean field. Different theories have been used to explain the smaller than expected transition temperature, a feature that is characteristic of all CDW materials.¹² One possibility is that the measured CDW transition temperature is strongly diminished from the mean-field value by $1-D$ fluctuations that are reduced at low applied pressures, while the gap is unaffected as it develops locally. In such a case, we would naturally expect to observe an increase of T_S at low pressures, due to the improvement of the coupling between ladders induced by pressure. Such a behavior has been observed in the one-dimensional compounds TaS_3 and $(\text{TaSe}_4)_2\text{I}$ (Ref. 13). Our observation of a monotonous decrease of T_S with pressure would thus indicate that one-dimensional fluctuations are not responsible for the reduction of T_S with respect of the mean-field value in $\text{Fe}_3\text{O}_2\text{BO}_3$. Therefore, the origin of this reduction should be the consequence of small fluctuations of the nesting wave vector that connect the interacting portions of

the Fermi surface^{3,14} or by strong inelastic scattering as suggested by Blawid and Millis.¹² With regard to the first hypothesis, we should note that the distortion wave vector seems to be connecting two different bands, i.e., a hole pocket on one band with an electron pocket of the other. Impurities such as oxygen vacancies can alter band filling locally, that will affect the actual distortion wave vector, and could be at the origin of the T_S reduction and possibly, of the incommensurations or domain walls detected in the ac-conductivity measurements. Also pressure increases the interladder interactions and facilitates the redistribution of charge carriers between them through an augmented Fe-O hybridization. Such a scenario has been proposed to explain the pressure dependence of the resistivity of the two-leg ladder compound $\text{Sr}_{1-x}\text{Ca}_x\text{Cu}_{24}\text{O}_{41}$.¹⁵

The pressure dependence of the critical temperature T_S shown in Fig. 6 is given by $T_S \approx |P - P_C|^y$ which also describes the variation of the conductivity gap. The critical pressure $P_C = 29.2$ GPa and the exponent $y = 0.6$, which incidentally is the same obtained for the charge-density-wave material,¹⁶ TaS_3 . However, no metallic nor superconducting state seems to be accessible in the present system for $T_S \rightarrow 0$, as is the case in TaS_3 .

We have presented dc-conductivity and ac-conductivity measurements in the charge-density-wave material

$\text{Fe}_3\text{O}_2\text{BO}_3$. This system contains subunits in the form of three leg ladders which dimerize in alternate directions perpendicular to the axis of the ladder. We have shown that the ac conductivity presents a characteristic frequency $\omega_0 \sim 10^{10}$ Hz, which is associated with defects or domain walls between symmetric charge-density-wave configurations and are affected by the oscillating electric field. We determined the effective mass of these defects that is approximately $10^5 - 10^4$ times the electron mass. This is slightly above the *Fröhlich mass* usually observed in conventional CDW systems.^{7,9} Different from these, however, we have found a large dielectric constant (in some cases larger than 1000) but in the direction *perpendicular* to the charge-density wave. The temperature of the structural instability and the gap in the conductivity decrease with pressure with the same power law.

ACKNOWLEDGMENTS

We wish to thank M. Avignon and P. Bordet for interesting discussions. We would like to thank the Brazilian agencies Conselho Nacional de Desenvolvimento Científico e Tecnológico-CNPq-Brasil (PRONEX98/MCT-CNPq-0364.00/00), Fundação de Amparo a Pesquisa do Estado do Rio de Janeiro-FAPERJ for partial financial support.

*Corresponding author. Electronic address: mucio@if.uff.br

¹M. Mir, R. B. Guimarães, J. C. Fernandes, M. A. Continentino, A. C. Doriguetto, Y. P. Mascarenhas, J. Ellena, E. E. Castellano, R. S. Freitas, and L. Ghivelder, *Phys. Rev. Lett.* **87**, 147201 (2001).

²See *Low Dimensional Electronic Properties of Molybdenum Bronzes and Oxides*, edited by C. Schlenker (Kluwer Academic Press, Netherlands, 1989).

³A. Latge and M. A. Continentino, *Phys. Rev. B* **66**, 094113 (2002).

⁴J. A. Larrea, D. R. Sanchez, E. M. Baggio-Saitovitch, R. B. Guimarães, J. C. Fernandes, M. A. Continentino, and F. J. Litterst, *Phys. Rev. B* **70**, 174452 (2004).

⁵R. B. Guimarães, M. Mir, J. C. Fernandes, M. A. Continentino, H. A. Borges, G. Cernicchiaro, M. B. Fontes, D. R. S. Candela, and E. Baggio-Saitovich, *Phys. Rev. B* **60**, 6617 (1999).

⁶M. Whangbo, H.-J. Koo, J. Dumas and M. A. Continentino, *Inorg. Chem.* **41**, 2193 (2002).

⁷See R. M. Fleming and R. J. Cava in Ref. 2, p. 259.

⁸See for example J. Beille, U. Beierlein, J. Dumas, C. Schlenker, and D. Groult, *J. Phys.: Condens. Matter* **13**, 1517 (2001).

⁹G. Grüner, *Rev. Mod. Phys.* **60**, 1129 (1988).

¹⁰J. C. Fernandes, R. B. Guimarães, M. A. Continentino, L. Ghivelder, and R. S. Freitas, *Phys. Rev. B* **61**, R850 (2000).

¹¹J. Dumas, J.-L. Tholence, M. A. Continentino, J. C. Fernandes, R. B. Guimarães, and M. H. Whangbo, *J. Phys. IV* **12**, 9-351 (2002).

¹²S. Blawid and A. Millis, *Phys. Rev. B* **62**, 2424 (2000).

¹³M. Nunez-Regueiro, J.-M. Mignot, M. Jaime, D. Castello, and P. Monceau, *Synth. Met.* **55-57**, 2653 (1993).

¹⁴W. L. McMillan, *Phys. Rev. B* **16**, 643 (1977).

¹⁵T. Nagata, M. Uehara, J. Goto, J. Akimitsu, N. Motoyama, H. Eisaki, S. Uchida, H. Takahashi, T. Nakanishi, and N. Mori, *Phys. Rev. Lett.* **81**, 1090 (1998).

¹⁶M. Monteverde, M. Nunez-Regueiro, P. Monceau, and F. Levy (unpublished).